Preliminary Site Investigation based on RGB Electromagnetic Energy of Landsat-7 Images in Wadi Fayidah, Saudi Arabia

Mohammed A. M. Alghamdi

Faculty of Earth Sciences, King Abdulaziz University, Jeddah, Saudi Arabia
mmushrif@kau.edu.sa
(corresponding author)

Adel Zein E. A. Bishta

Faculty of Earth Sciences, King Abdulaziz University, Jeddah, Saudi Arabia
abishta@kau.edu.sa

ABSTRACT

In this paper, geostatistical analysis of digital image processing data efficiently contributed to the preliminary site investigation and geotechnical mapping of Wadi Fayidah, Saudi Arabia. 3D modeling, clustering, and chart pattern changes were used to analyze the spectral electromagnetic energy reflected values in red, green, and blue (RGB) ranges on false color composite Landsat-7 images. Therefore, from upstream to downstream, a series of measurements were carried out on a 70km dendritic drainage pattern at 78 stations. Wadi Fayidah was found to have a dominant structural lineament of 56° to 84°. Furthermore, as a preliminary engineering geology mapping, Wadi Fayidah has 9 lithofacies that may differ in engineering geological properties.

Keywords-structural lineaments; lithofacies; statistical analysis; image processing

I. INTRODUCTION

Site investigation is an essential step in any engineering project in order to identify and quantify ground conditions affecting a structure's viability, design, or construction. As a preliminary site investigation tool, remote sensing aims to acquire a general engineering geological understanding of the project area or site. Hence, it gathers information about lithology, structure, and geomorphology without physical contact [1]. Remote sensing and digital image processing techniques are essential in mineral and groundwater exploration, lithological discrimination, and structural mapping [2]. Remote sensing, high-resolution imagery, and GIS have become essential tools for locating and selecting the best sites of mineral deposits by detecting the locations of alteration zones [3]. The mineral deposits usually occur along or are adjacent to the geologic structures and alteration mapping, as mineral deposits are commonly associated with hydrothermal alteration of the surrounding rocks [4-5]. Image processing of digital data has been used for lithological and structural interpretation [6-11]. Authors in [12] used remote sensing techniques for geological mapping. Authors in [13] utilized Landsat images to assess construction materials, while authors in [14] employed statistics and enhanced RGB images in surface water interpretation. The differences in soil color from an RGB camera were investigated at different distances, times, and illumination levels obtained from loam soil over four weeks of data acquisition [15]. Authors in [16] studied Munsell's soft color and soil reflectance in the visible spectral bands of Landsat MSS and TM Data. RGB values appear to be strongly correlated with the soil reflectance measured in the corresponding spectral bands of Landsat sensors.

As a different approach for a preliminary site investigation of Wadi Fayidah, this work uses geostatistical analysis such as 3D modeling, clustering, and phenomena chart tracking of Landsat-7 ETM+ (Enhanced Thematic Mapper Plus) digital satellite data. Consequently, this study aims to achieve a method of interpreting drainage patterns, structural lineaments, and lithofacies. The aim is to produce an engineering special-purposed geological map.

II. GEOLOGICAL SETTING

Wadi Fayidah is located in the Northern Makah region, between latitudes 21°50' and 21°59'N and longitudes 39°20' and 39°55 E (Figure 1). The investigated area belongs to the Arabian Shield, shielded by Precambrian metasediments and metavolcanics. These rocks are covered by Quaternary sediments and intruded by dioritic rocks. It is a basin among the deformed, weakly metamorphosed, post-amalgamation volcano-sedimentary sequence in the Arabian Shield, Saudi Arabia [17].
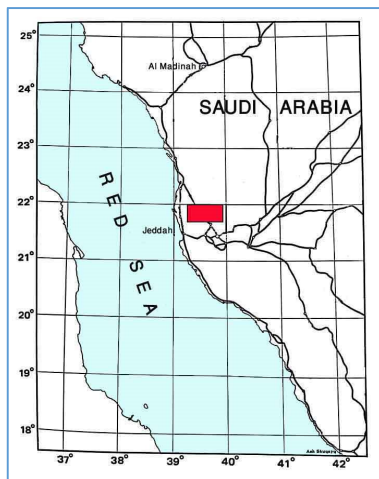
Fig. 1.   Location map.

Fig. 2.   Graphical abstract of the workflow.

According to [18], the geology of Wadi Fayidah falls into four groups: (1) Proterozoic crystalline basement, (2) Tertiary sedimentary rocks, (3) Tertiary volcanic rocks, and (4) Quaternary sediments. The Proterozoic basement comprises volcanic and volcano-sedimentary formations of various ages and compositions, intruded by plutons of diverse composition but with strong granodiorite affinities. Tertiary sedimentary rocks consist of Shumaysi, Khulays, and Khulaysiyah [18, 20] and Hammar formation [21]. It comprises Tertiary clastic and carbonates rocks that crop out over a minimal area. However, they are thought to underlie the Quaternary sediments and Late Tertiary basalts in much of Wadi as Sukkah (As Suqah), Wadi al Aghran, and the coastal plain [21]. The Shumaysi to Ubhur formations has been tilted, faulted, and linked to the significant Red Sea rifting [21].

III. METHODOLOGY

The multispectral digital satellite data of Landsat-7 ETM+ were downloaded from the USGS website. They were radiometric and geometrically corrected to UTM 37N (WGS-84 datum) by the USGS EROS Center. This information is used for regional geotechnical surveys of the study area. Advanced remote sensing software such as ERDAS Imagine and PCI Geomatica provide various image-processing techniques such as geometric correction and image enhancement. This study uses digital image processing techniques with the statistical analysis of digital satellite data. A geometric correction has been applied to the data because geometric errors are caused by the sensor or scanner's geometry, the earth's curvature and rotation, etc. [22]. These data (Landsat-7 ETM+) comprise bands B1-B3 (visible rays), bands B4, B5, and B7 (infrared rays), band B6 (thermal rays), and a panchromatic band (B8). These bands are of 30m spatial resolution except band 6 (60m) and band 8 (15m). In addition, to make the processed images interpretable, histogram equalization and smooth filtering were applied [22]. The geostatistical analysis of the extracted lineaments, visible green enhancement band (EG), and the digital number (DN) values of RGB pixels (Landsat ETM+ bands 7, 4, 2, in red, green, and blue, respectively), along Wadi Fayidah, are summarized in the flow-chart approach shown in Figure 2.
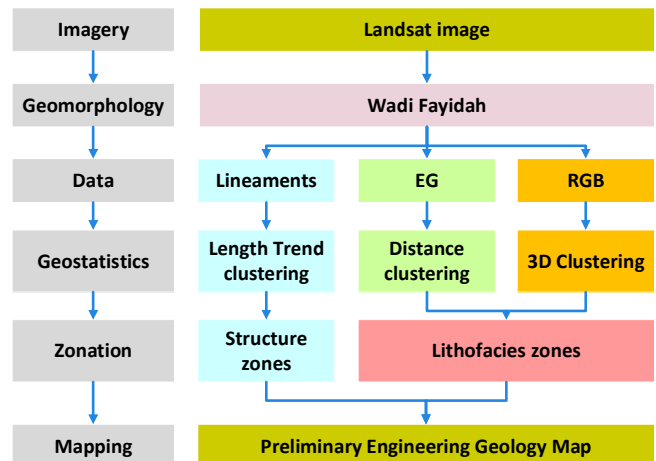
Landsat-7 ETM+ digital data were processed to yield a False-Color Composite (FCC) image on a scale of 1:100000. The best band combination obtained for this FCC image consists of ETM band 7 (SWIR), band 4 (NIR), and band 2 (visible green) in RGB, based on the selection of the most significant variance bands with the minor correlation. In addition, it shows a regional view of the study area, the main rock units, and Wadies. The Landsat images cover a large area (185 by 170km) and illustrate its regional geology and topography. Extraction of lineaments from the digital Landsat data is carried out to show the structural analysis of the Wadi Fayidah area. It is also very useful in the seismic and risk of landslide evaluation [22]. Lineaments usually reflect linear structural features in the rocks or artificial features like roads or buildings. Lineament extraction is usually carried out by using digital data of satellite either manually [23-24] or automatically [25-26]. The automatic lineament extraction technique is applied in this work to interpret and extract the structural lineaments from the digital SPOT-5 data of the study area.

IV. RESULTS

Seventy-eight stations were placed at spaced distances (about 70Km long) with the Wadi Fayidah. These stations begin at the highest valley (upstream) on the east and end at the mouth of the Wadi (downstream) on the west (Figure 3). The statistical analysis of the relationship between interfaces, distance separations, and frequencies (the total number of stations in each distance) was carried out. Figure 4 shows the normal distribution of a histogram of the relationships between the distance separations between stations and their frequencies. Each station has taken various measurements, such as location coordinates and RGB spectral values of Landsat color composite images for raw and enhancement data in the three bands (bands 7, 4, and 2, in red, green, and blue). In addition, rock type, geomorphological type, and the trends and lengths of the structural lineaments were also taken at each station (Figure 5).

Table I describes the lithologic unit types in the 78 stations along Wadi Fayiddah. The symbols and descriptions of the lithologic units with their codes (arranged from 1-the oldest rock units to 23-the youngest rock units) are also listed.
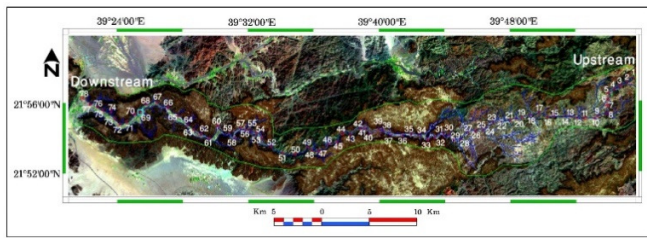
Fig. 3.   Locations of the 78 stations along Wadi Fayidah, on false color composite Landsat image.
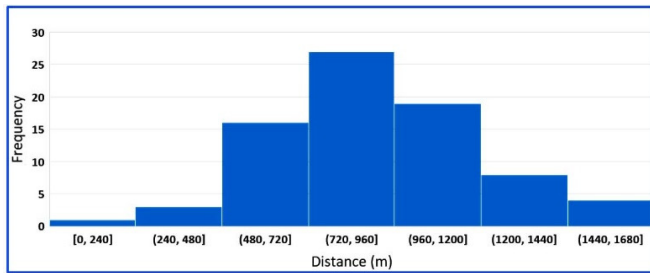

Fig. 4.   Frequencies of the distance separations between stations.

Fig. 5.   Some RGB data acquired from the Landsat image on the 78 stations along Wadi Fayidah.

TABLE I.   LITHOLOGICAL UNIT TYPES OF THE 78 STATIONS ALONG WADI FAYIDAH

Station No.	Rock Type		
	Symbol	Code	Description
1-5	ibmv-p€	2	Meta-Andesitic to Metabasaltic
6-8	todr-p€	11	Tonalite
9-11	gr-p€	13	Granite
12-14	gdmo-p€	12	Granodiorite
15-18	mdgb-p€	1	Metadiorite and Gabbro
19-32	todr-p€	11	Tonalite
33-35	sscg-t	15	Sandstone and Conglomerate
36	ss-t	16	Sandstone and Oolitic iron ore
37	sscg-t	15	Sandstone and Conglomerate
38-51	ibvs-p€s	3	Samran group, Volcanosedimentary rocks
52-54	sscg-t	15	Sandstone and Conglomerate
55	ibvs-p€s	3	Samran group, Volcanosedimentary rocks
56, 57	gv-Q	22	Gravel
58, 59	sscg-t	15	Sandstone and Conglomerate
60	gv-Q	22	Gravel
61 to 78	clss-t	14	Clay, sandstone and tuff

V.   ANALYSIS AND DISCUSSION

The study area's Landsat-7 color composite images (bands 7, 4, 2 in RGB) were processed. The study area is dissected by

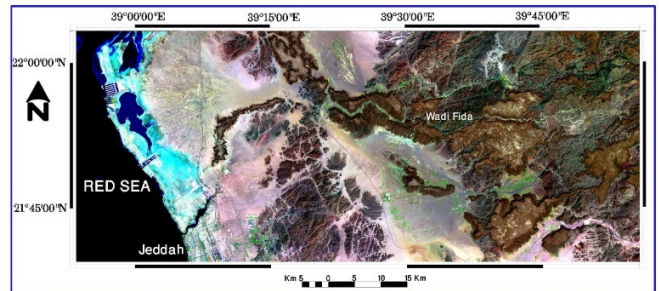some significant Wadies running from the East to the West, as shown in Figure 6.

Fig. 6.   False color composite Landsat-7 ETM+ image, showing Wadi Fayidah area.

A. Drainage

The image processing technique was applied to extract a subset of the false color composite Landsat image for the exact boundary of Wadi Fayidah Basin, as shown in Figure 7.

Fig. 7.   False color composite Landsat-7 ETM+ image of Wadi Fayidah Basin.

Figure 8 shows the dendritic drainage pattern of Wadi Fayidah as interpreted from the FCC Landsat-7 ETM+ image in Figure 7. The Wadi Fayidah is one of the longest, more than 70km long, Wadies in the area. A dendritic drainage pattern that looks like the branching pattern of tree roots develops in regions underlain by homogeneous material. The availability of this pattern reflects the similarity of resistance to weathering, so there is no apparent control over the direction the tributaries take.

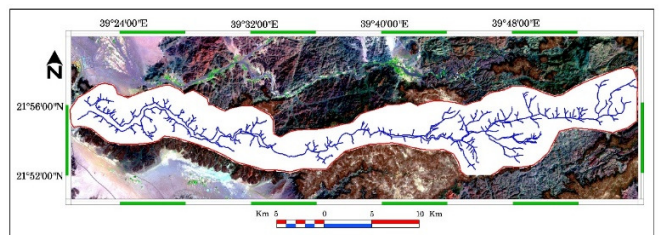Fig. 8.   The dendritic drainage pattern of Wadi Fayidah.

B. Lithofacies

As illustrated in Figure 5, numerous variables were measured at the 78 stations for classification purposes. The statistical analysis was performed in three steps.

1) Step-1: 3D Visual RGB Clustering

Figure 9 shows the 3D layout of the raw data's Red, Green, and Blue bands. The plotting indicates that the data can be

categorized into two groups. The stations of the first category were clogged on the map with yellow color (Figure 10). In addition, it was observed that stations located close to each other, are classified as one zone with the same lithofacies properties. Therefore, the study area can be categorized into two zones with different lithological properties.
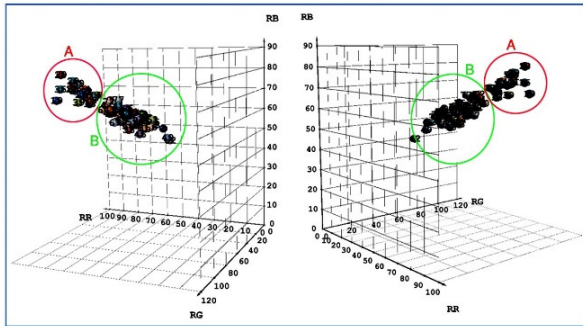

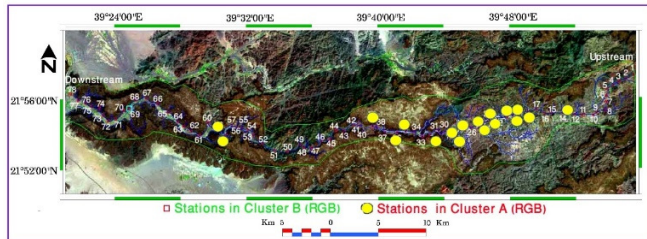Fig. 9. Two views of the same 3-D plot showing two RGB clusters (A and B).

Fig. 10. The first cluster of 3D RGB stations (yellow color).

2) Step-2: EG (Enhancement Green) Fluctuation

The EG spectrum was selected to reflect the highest intensity and reflectance compared to other spectra. Based on the different properties from one location to another, the change in EG values is shown in Figure 11. It offers three distinct clusters. These categories are discriminated in the profile and satellite image as Zone-I, Zone-II, and Zone-III (Figure 12).
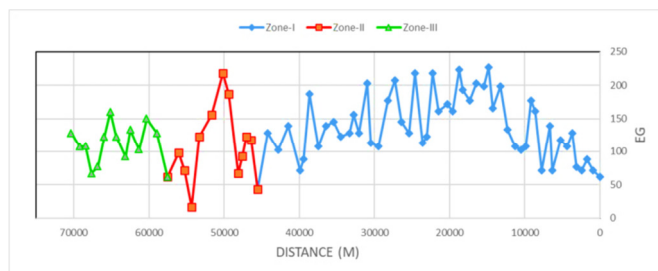

Fig. 11. EG profile through distance, along Wadi Fayidah.

3) Step-3: EG and 3D_RGB Merging

After merging the RGB clusters and the EG zones, Wadi Fayidah can be categorized into 7 zones. Each zone depicts different lithofacies, which may reflect different engineering

properties. Alternatively, this classification will organize the sampling area rather than reducing or expanding it.
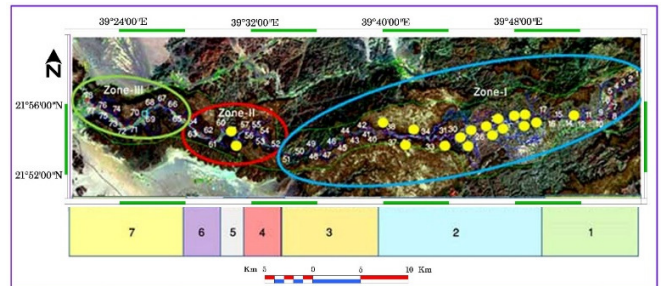

Fig. 12. Zones of EG fluctuation (blue, red, and green ellipses).

C. Lineaments

Automatic lineament extraction was carried out from the digital data of FCC Landsat image of Wadi Fayidah basin. Visual editing was done to delete the false lines (not structural lines) for the extracted lineaments to construct the Wadi Fayidah basin's structural lineaments, as shown in Figure 13. It was interpreted from a False color composite Landsat-7 ETM+ image.
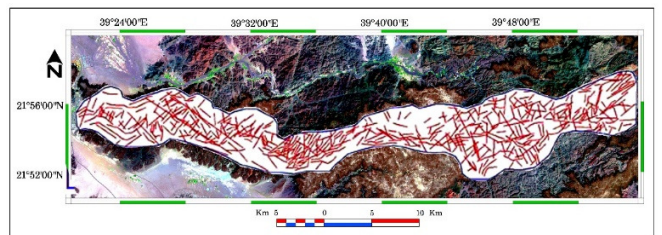
Fig. 13. Structural lineament map of Wadi Fayidah area.

Figure 14 illustrates the relationship between the structural lineaments (frequency) and trend ranges. It concludes that Wadi Fayidah's dominant structure tends to be between 56° and 84°. The relationships between the directions of the lineament's structure (X-axis) and their lengths (Y-axis) are shown in Figure 15, which reflects the availability of two lineament clusters.

Fig. 14. Histogram of the predominant structural lineaments trend.

Fig. 15.   Structural lineament evaluation of Wadi Fayidah.

Both clusters offer a positive relationship between length and direction. However, the first cluster, which covers fewer stations, shows more significant lengths than the second one. Otherwise, the trends in the first cluster are limited compared to the second cluster. The second cluster co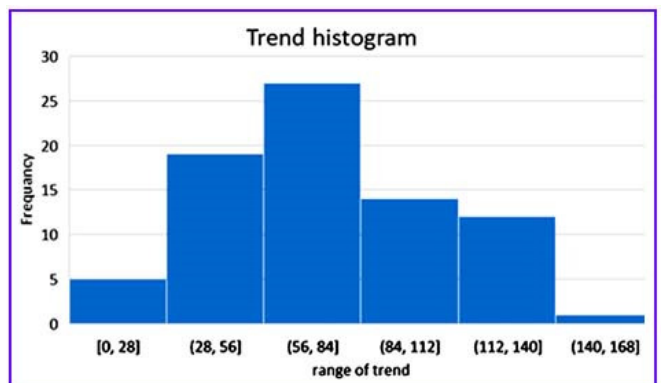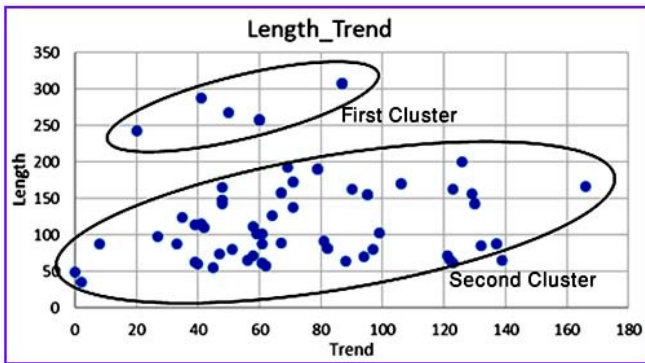vers most stations in Wadi Fayidah. It has shorter lengths, with greater directions than the first one. Generally, the second cluster trend is predominant in the Wadi Fayidah. The relationship between the length and azimuth of the structural lineaments is positive. From a geology engineering point of view, keeping the construction far from the structure locations and short length of constructions walls or foundation perpendicular to lineament trends is recommended. Circular or curved design may also be recommended for equality stress distribution.

In a lineament structure of about 200m long, the study area can reflect two zones, as sown in Figure 15. The remaining shorter lineaments will cover the other stations. So, if these 2 zones are added to the previous 7 zones, we get 9 engineering geological zones (Figure 16).
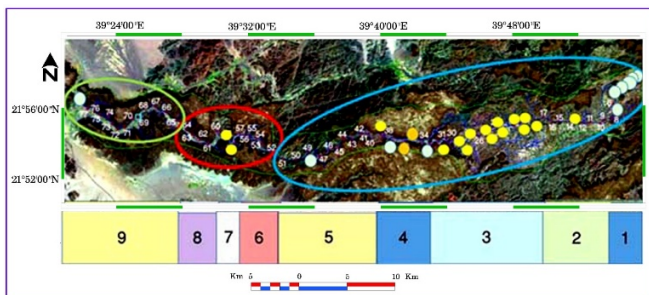

Fig. 16.   Zones of the study area.

D. Engineering Geological Mapping

To ensure that the approach used in this document is practical, the analysis and interpretation of the Landsat images were compared with the geological map of [21]. It was found that the 9 zones explored through this research match the changes in rock types of [21]. Table II summarizes the lithofacies and structure length of each zone. Consequently, an engineering geological map was introduced (Figure 17).

Previous works, such as the applicability of Landsat-8 and regression analysis in developing models for estimating water

quality parameters explored in [14], did not utilize the beneficial approach used in the current research, i.e. the RGB spectral value characterization of Landsat ETM+ data and the clustering method in the 3-D plot of the RGB data, to classify and identify the spectral enhanced data into different zones. The current study produced an engineering geological map with 9 lithofacy zones in Wadi Fayidah. To the best of our knowledge, the technique of RGB electromagnetic energy processing is presented in this study for the first time.

TABLE II.   LITHOLOGICAL UNIT TYPES OF THE 9ZONES ALONG WADI FAYIDAH

| Zone No.	Stations (St.)	No of St.	Rock Type			Structure
			Symbol	Code	Description	Length
Zone-1	1-8	9	ibmv-p€ todr-p€	2	Meta-Andesitic to metabasaltic Tonalite	≥ 200 m
Zone-2	9-16	8	gdmo-p€ gr-p€	12	Granodiorite Granite	≤ 200 m
Zone-3	17-32	16	todr-p€	11	Tonalite	≤ 200 m
Zone-4	33-39	7	sscg-t sssh-t	15	Sandstone and Conglomerate	≥ 200 m
Zone-5	40-51	12	ibvs-p€s	3	Samran group, Volcanosedimentary rocks	≤ 200 m
Zone-6	52-56	5	sscg-t	15	Sandstone and Conglomerate	≤ 200 m
Zone-7	57-59	3	Gdma-p ss-t		Granodiorite Sandstone and Oolitic iron ore	≤ 200 m
Zone-8	60-64	5	clss-t	14	Clay, sandstone and tuff	≤ 200 m
Zone-9	65-78	14	clss-t	14	Clay, sandstone and tuff	≤ 200 m
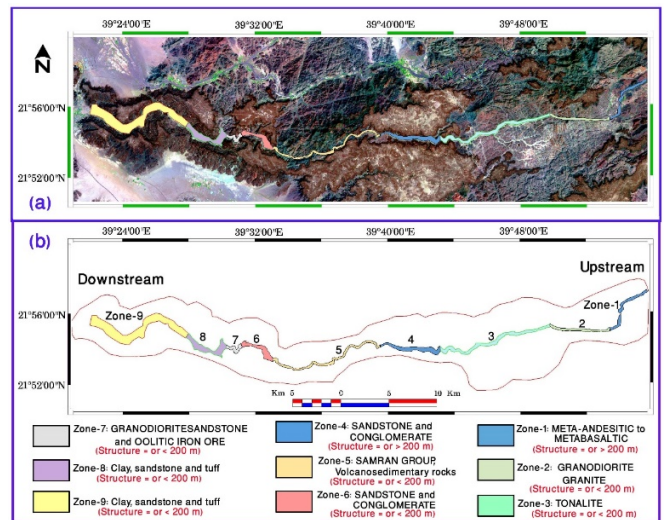
Fig. 17.   Engineering geological map showing the 9 lithofacy zones of Wadi Fayidah (a) Landsat image view, (b) clear view.

VI.   CONCLUSION

Based on Landsat-7 RGB electromagnetic energy and statistical data analysis, Wadi Fayidah has been primarily investigated for engineering geological purposes in this paper. The resulting conclusions of the current research are:

- With a length of 70km from upstream to downstream, Wadi Faydah is classified as a dendritic drainage pattern that reflects the similarity of resistance to weathering for the subsurface.

- The primary trend of the lineament structure of Wadi Fayidah ranges between 56° and 84°.

- Based on geology, structural lineaments, and RGB analysis, Wadi Fayidah is classified into 9 different lithofacies.

- For more emphasis on validity and reliability, applying the geostatistical analysis approach to RGB data in other studies is recommended.

REFERENCES

[1] L. G. de Vallejo and M. Ferrer, *Geological Engineering*. London, UK: CRC Press, 2011.

[2] F. F. Sabins, *Remote Sensing: Principles and Interpretation*, 2nd ed. New York, NY, USA: W. H. Freeman and Company, 1986.

[3] A. R. Sonbul, M. K. El-Shafei, and A. Z. Bishta, "Using remote sensing techniques and field-based structural analysis to explore new gold and associated mineral sites around Al-Hajar mine, Asir terrane, Arabian Shield," *Journal of African Earth Sciences*, vol. 117, pp. 285–302, May 2016, https://doi.org/10.1016/j.jafrearsci.2016.02.009.

[4] A. Bishta, "Assessing Utilization of Multi-Resolution Satellite Imageries in Geological Mapping, A Case Study of Jabal Bani Malik Area, Eastern Jeddah City, Kingdom of Saudi Arabia," *Journal of King Abdulaziz University : Earth Sciences*, vol. 21, Jan. 2010.

[5] A. Z. Bishta and A. R. Sonbul, "Supervised Classification and Lineaments Extraction of SPOT-5 Imageries in the Geological Mapping of Kutaina–Al Hajar Area, Arabian Shield, Saudi Arabia," *Life Science Journal*, vol. 12, no. 11, pp. 80–92, 2015.

[6] A. Z. Bishta, "Assessment of the reliability of supervised classifications of Landsat-7, ASTER, and SPOT-5 multispectral data in rock unit discriminations of Jabal Daf-Wadi Fatima area, Saudi Arabia," *Arabian Journal of Geosciences*, vol. 11, no. 23, Dec. 2018, Art. no. 755, https://doi.org/10.1007/s12517-018-4093-2.

[7] S. S. Gabr, S. M. Hassan, and M. F. Sadek, "Prospecting for new gold-bearing alteration zones at El-Hoteib area, South Eastern Desert, Egypt, using remote sensing data analysis," *Ore Geology Reviews*, vol. 71, pp. 1–13, Dec. 2015, https://doi.org/10.1016/j.oregeorev.2015.04.021.

[8] Y. Ding, K. Zhao, X. Zheng, and T. Jiang, "Temporal dynamics of spatial heterogeneity over cropland quantified by time-series NDVI, near infrared and red reflectance of Landsat 8 OLI imagery," *International Journal of Applied Earth Observation and Geoinformation*, vol. 30, pp. 139–145, Aug. 2014, https://doi.org/10.1016/j.jag.2014.01.009.

[9] H. A. Alanazi and H. A. Ghrefat, "Spectral Analysis of Multispectral Landsat 7 ETM + and ASTER Data for Mapping Land Cover at Qurayah Sabkha, Northern Saudi Arabia," *Journal of the Indian Society of Remote Sensing*, vol. 41, no. 4, pp. 833–844, Dec. 2013, https://doi.org/10.1007/s12524-013-0291-2.

[10] J. R. Irons, J. L. Dwyer, and J. A. Barsi, "The next Landsat satellite: The Landsat Data Continuity Mission," *Remote Sensing of Environment*, vol. 122, pp. 11–21, Jul. 2012, https://doi.org/10.1016/j.rse.2011.08.026.

[11] R. Amer, T. Kusky, and A. Ghulam, "Lithological mapping in the Central Eastern Desert of Egypt using ASTER data," *Journal of African Earth Sciences*, vol. 56, no. 2, pp. 75–82, Feb. 2010, https://doi.org/10.1016/j.jafrearsci.2009.06.004.

[12] M. K. Villareal and A. F. Tongco, "Remote Sensing Techniques for Classification and Mapping of Sugarcane Growth," *Engineering, Technology & Applied Science Research*, vol. 10, no. 4, pp. 6041–6046, Aug. 2020, https://doi.org/10.48084/etasr.3694.

[13] M. A. M. Alghamdi, "Suitability of Quaternary Sediments of Wadi Arar, Saudi Arabia, as Construction Materials: An Environmental Radioactivity Approach," *Engineering, Technology & Applied Science Research*, vol. 9, no. 5, pp. 4735–4740, Oct. 2019, https://doi.org/10.48084/etasr.3039.

[14] M. V. Japitana and M. E. C. Burce, "A Satellite-based Remote Sensing Technique for Surface Water Quality Estimation," *Engineering, Technology & Applied Science Research*, vol. 9, no. 2, pp. 3965–3970, Apr. 2019, https://doi.org/10.48084/etasr.2664.

[15] A. Al-Naji, A. B. Fakhri, S. K. Gharghan, and J. Chahl, "Soil color analysis based on a RGB camera and an artificial neural network towards smart irrigation: A pilot study," *Heliyon*, vol. 7, no. 1, Jan. 2021, Art. no. e06078, https://doi.org/10.1016/j.heliyon.2021.e06078.

[16] R. Escadafal, M.-C. Girard, and D. Courault, "Munsell soil color and soil reflectance in the visible spectral bands of landsat MSS and TM data," *Remote Sensing of Environment*, vol. 27, no. 1, pp. 37–46, Jan. 1989, https://doi.org/10.1016/0034-4257(89)90035-7.

[17] U. S. Hargrove, R. J. Stern, J.-I. Kimura, W. I. Manton, and P. R. Johnson, "How juvenile is the Arabian–Nubian Shield? Evidence from Nd isotopes and pre-Neoproterozoic inherited zircon in the Bi'r Umq suture zone, Saudi Arabia," *Earth and Planetary Science Letters*, vol. 252, no. 3, pp. 308–326, Dec. 2006, https://doi.org/10.1016/j.epsl.2006.10.002.

[18] C. H. Spencer and P. L. Vincent, *Bentonite resources potential and geology of Cenozoic sediments, Jeddah region. Open File Report BRGM-OF-04-31 (1984)*. Saudi Arabia: Saudi Arabia Deputy Ministry for Mineral Resources, 1984.

[19] D. G. Hadley and R. J. Fleck, "Reconnaissance Geologic Map of the Al Lith Quadrangle, Sheet 20/40 C, Kingdom of Saudi Arabia. Scale 1:100000," 1980.

[20] D. L. Schmidt, D. G. Hadley, and G. F. Brown, "Middle Tertiary continental rift and evolution of the Red Sea in southwestern Saudi Arabia," US Geological Survey, Reston, VA, USA, USGS Numbered Series 83–641, 1983, https://doi.org/10.3133/ofr83641.

[21] C. H. Spencer, A. Cartier, and P. L. Vincent, *Industrial mineral resources map of Jiddah, Kingdom of Saudi Arabia*. Saudi Arabia: Saudi Arabia Deputy Ministry for Mineral Resources, 1988.

[22] T. Lillesand, R. W. Kiefer, and J. Chipman, *Remote Sensing and Image Interpretation*, 7th ed. Hoboken, N.J, USA: Wiley, 2015.

[23] M. L. Suzen and V. Toprak, "Filtering of satellite images in geological lineament analyses: An application to a fault zone in Central Turkey," *International Journal of Remote Sensing*, vol. 19, no. 6, pp. 1101–1114, Jan. 1998, https://doi.org/10.1080/014311698215621.

[24] E. E. Nama, "Technical note: Lineament detection on Mount Cameroon during the 1999 volcanic eruptions using Landsat ETM," *International Journal of Remote Sensing*, vol. 25, no. 3, pp. 501–510, Feb. 2004, https://doi.org/10.1080/0143116031000102557.

[25] M. E. Mostafa and A. Z. Bishta, "Significance of lineament patterns in rock unit classification and designation: a pilot study on the Gharib-Dara area, northern Eastern Desert, Egypt," *International Journal of Remote Sensing*, vol. 26, no. 7, pp. 1463–1475, Apr. 2005, https://doi.org/10.1080/01431160410001705088.

[26] N. Vassilas, S. Perantonis, E. Charou, T. Tsenoglou, M. Stefouli, and S. Varoufakis, "Delineation of Lineaments from Satellite Data Based on Efficient Neural Network and Pattern Recognition Techniques," in *2nd Hellenic Conf. on AI, SETN-2002, 11-12 April 2002, Thessaloniki, Greece, Proceedings, Companion Volume*, Apr. 2022, pp. 355–366.